Virchows Arch [Cell Pathol] (1983) 44:355–368

Virchows Archiv B

Tilorone-induced lysosomal storage mimicking the features of mucopolysaccharidosis and of lipidosis in rat liver

Renate Lüllmann-Rauch
Anatomisches Institut der Universität Kiel, Olshausenstr. 40–60, D-2300 Kiel, Federal Republic of Germany

Summary. This ultrastructural and histochemical study deals with the lysosomal storage phenomena occurring in the rat liver after repeated oral administration of tilorone, an agent with anti-tumor and anti-viral activities. In the sinusoidal endothelium and in Kupffer cells, the lysosomes were changed into large vacuoles which contained material with the histochemical characteristics of acid glycosaminoglycans. The alterations closely resembled those previously observed in the splenic red pulp of tilorone-treated rats. In hepatocytes, the lysosomes were converted into large multilamellated inclusions indicating storage of polar lipids. The results show that, in the rat liver, tilorone induces cellular alterations mimicking those of inherited mucopolysaccharidoses and lipidoses. After discontinuing drug treatment the two storage phenomena gradually faded at different rates: The lipidosis disappeared within 2 to 4 weeks, whilst mucopolysaccharidosis-like changes were still found 15 weeks after drug withdrawal.

The occurrence of lipidosis is not surprising, since by its molecular structure tilorone can be regarded as belonging to the group of amphiphilic cationic drugs which often have this side effect. Much more surprising is the occurrence of mucopolysaccharidosis-like alterations. The exact biochemical identification of the polyanionic storage material and the molecular mechanisms responsible for this drug side effect remain to be established.

Key words: Acid Glycosaminoglycans – Mucopolysaccharidosis – Lysosomes – Tilorone – Rat liver

Introduction

Tilorone (Fig. 1) is a drug which stimulates interferon production and has anti-viral and anti-tumor activities (Regelson 1981). Among its cytological side effects there are two which involve the lysosomes: (a) tilorone induces

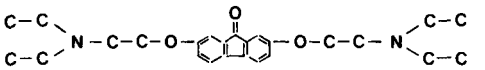

Fig. 1. Molecular structure of tilorone depicted as the free base; the C-bound H-atoms are omitted. Due to the presence of an apolar ring system and two short side chains with protonizable nitrogens tilorone can be regarded as an amphiphilic cationic compound

lamellated cytoplasmic inclusions in hepatocytes and renal tubular cells of animals (Leeson et al. 1976; Thelmo and Levine 1978) and in corneal epithelium of humans (Weiss et al. 1980); this side effect presumably reflects lipidosis which can also be produced by many other cationic amphiphilic drugs (Lüllmann-Rauch 1979). (b) Tilorone induces cytoplasmic vacuolation in several cell types (Levine and Sowinski 1977; Thelmo and Levine 1978); histochemical findings have recently provided evidence that the clear vacuoles occurring in the splenic sinus endothelium are due to excessive lysosomal storage of acid glycosaminoglycans (aGAG) (Lüllmann-Rauch 1982a) thus mimicking the cytological picture of inherited mucopolysaccharidoses (Van Hoof 1973). The purpose of this study was to examine whether mucopolysaccharidosis-like alterations are a more generalized phenomenon occurring also in the liver of tilorone-treated rats.

Materials and methods

Young adult female Wistar rats were used in all experiments. Tilorone-HCl was a gift of Merrell Dow Pharmaceuticals (Cincinnati, Ohio). The following dyes were used for histochemical work: toluidine blue 0 (Merck, Darmstadt, FRG); Alcian blue 8 GX (Gurr; Hopkin & Williams, Chadwell Heath, GB). Most experimental animals and procedures were the same as those described in detail in a previous study (Lüllmann-Rauch 1982a). Briefly, rats were treated (3–21 weeks) with tilorone-HCl at daily dosages of 60–80 mg/kg; the drug was added to the diet. Additional rats received higher drug doses by stomach tube (3 to 4×300 mg/kg within 8 days). Age-matched controls were kept under identical conditions without receiving the drug. To test the reversibility of the cellular alterations, 2 rats were allowed to survive without drug treatment for 2 and 4 weeks, respectively, following drug treatment for 4 weeks; 3 other rats were allowed to survive for 4, 7 and 15 weeks, after treatment for 13 weeks.

At the end of the experiments, animals were anaesthetized with pentobarbital and usually killed by vascular perfusion with glutaraldehyde. All methods for routine morphology and ultrastructural enzyme histochemistry (demonstration of acid phosphatase by means of Gomori's medium) were the same as described previously (Lüllmann-Rauch 1982a). In addition, demonstration of another lysosomal enzyme, trimetaphosphatase, was performed (Doty et al. 1977; Oliver 1980). Semithin Araldite sections were stained with toluidine blue-pyronin at alkaline pH (Ito and Winchester 1963); ultrathin sections were stained with uranyl acetate and lead citrate.

Substrate histochemistry. Most histochemical preparations of liver tissue were obtained in the same experiments previously described when the spleen was investigated (Lüllmann-Rauch 1982a); thus a direct comparison between the two organs was possible. Briefly, air-dried cryostat sections of unfixed tissue were stained with 1% Alcian blue at pH 1 (0.1 N HCl) or with 0.1% toluidine blue at pH 2 (Michaelis buffer) and mounted with DePeX. It should be mentioned that in recent experiments, where we used a new batch of toluidine blue, the metachromatic staining of certain structures including mast cells was converted to blue during

the last stage of dehydration with ethanol. Thus the toluidine blue preparations had to be mounted with gelatine which required their immediate evaluation since complete fading of the stain occurred within days. High iron diamine staining (HID) according to Spicer et al. (1978), and determination of the "critical electrolyte concentration" of alcianophilia (Scott and Dorling 1965) were performed by using 40 µm vibratome-slices of glutaraldehyde-fixed liver tissue, with cartilage and mast cells (tracheal wall) serving as internal standards for the latter method (Lüllmann-Rauch 1982a). PAS-staining was performed in two ways: (a) Araldite sections of freeze-dried, osmicated liver tissue (see below) were stained according to McManus (Pearse 1961), without removal of the Araldite; the periodic acid step was therefore prolonged to 2 h. (b) Rats were starved for 18 h prior to sacrifice in order to reduce the background staining due to glycogen in the hepatocytes; cryostat sections of unfixed liver tissue were treated with 90% ethanol (10 min), following which the PAS method was applied in a similar fashion to that recommended by Hotchkiss (Pearse 1961) for water-soluble materials, by performing the periodic acid step (2 h) in 90% ethanol buffered with 0.2 M sodium acetate.

Extraction and enzyme digestion experiments. Extractability of the Alcian blue positive material was tested by incubating air-dried cryostat sections of unfixed tissue for 2 h (20° C) in methanol (100%), chloroform/methanol (2:1), chloroform/methanol/water (4:8:3), or in saline (0.9% NaCl solution). In an attempt to preserve the water-soluble material from complete extraction in saline, cryostat sections were pretreated either with paraformaldehyde vapour (60° C, 60 min), or with methanol/formalin/acetic acid (85:10:5, 10 min) according to Mayrhofer (1980); the former was without effect, the latter was able to preserve some material during a subsequent saline incubation for 2 h at 20° C, but not at 37° as required for digestion experiments with hyaluronidase. Thus the classical approach to characterize a material by its enzyme digestibility was not possible.

Further attempts to test the digestibility of the storage material were made without success and are therefore described briefly here: (a) since Alcian blue (pH 1) and toluidine blue (pH 2) obviously stained and precipitated the storage materials in cryostat sections, and since complexes of glucosaminoglycans with such cationic dyes are poorly water-soluble (Scott et al. 1964), we tried to use the above dyes as "fixatives" prior to enzyme digestion experiments. As a positive control, cryostat sections of unfixed tracheal cartilage were included. The results were as follows: toluidine blue (pH 2) faded and was ineffective in preserving the storage material and the cartilagineous matrix during saline incubation (37° C, 180 min). Pretreatment with Alcian blue (pH 1) did preserve the storage material and the cartilagineous matrix but made the latter undigestible by hyaluronidase (from bovine testes, Sigma type IV). The hyaluronidase technique as such (enzyme 2,000 units/ml 0.9% NaCl solution, 3 h, 37° C) had been controlled before by use of cartilage cryostat sections fixed with paraformaldehyde vapour. (b) Freeze-dried samples of liver and trachea were embedded in Araldite, either after osmication (OsO_4-vapour, 2 h, 65° C) or without osmication. Before the hyaluronidase experiment, Araldite had to be removed with NaOH-ethanol as described previously (Lüllmann-Rauch 1982b). During this procedure the storage material was lost from the sections of non-osmicated tissue blocks. In the osmicated preparations, the storage material was retained during Araldite removal; however, osmication rendered the cartilagineous matrix undigestible. Therefore this procedure was regarded as unsuitable for enzyme digestion experiments.

Endocytosis experiments. Two rats treated with tilorone for 3 and 21 weeks, respectively, and age-matched control rats were used. They received a single intravenous injection of iron dextran (Myofer 100, Hoechst, Frankfurt, FRG). The amount of tracer injected corresponded to 5 mg iron per 100 g body weight in one experiment, and to 10 mg iron in the other. The animals were fixed by perfusion 4 days and 24 h, respectively, after the injection. For light microscopic demonstration, semithin sections were treated with NaOH-ethanol to remove the Araldite and were stained with Turnbull's blue and Safranin. Ultrathin sections were viewed unstained.

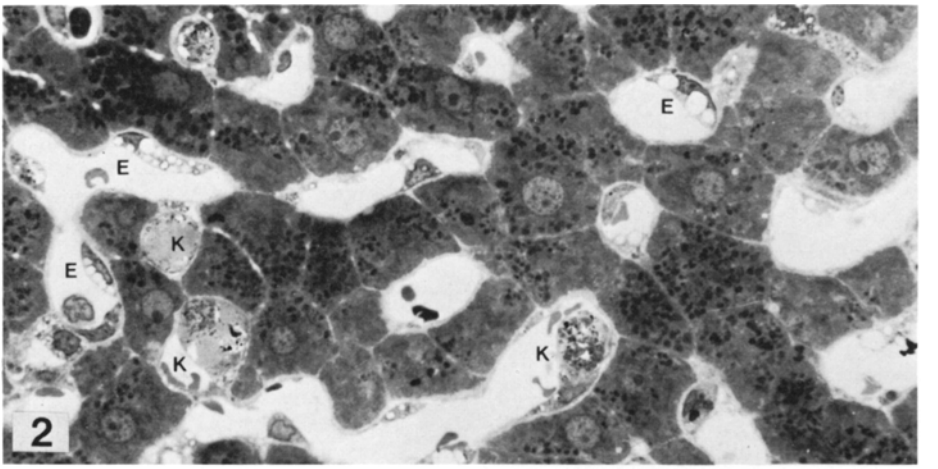

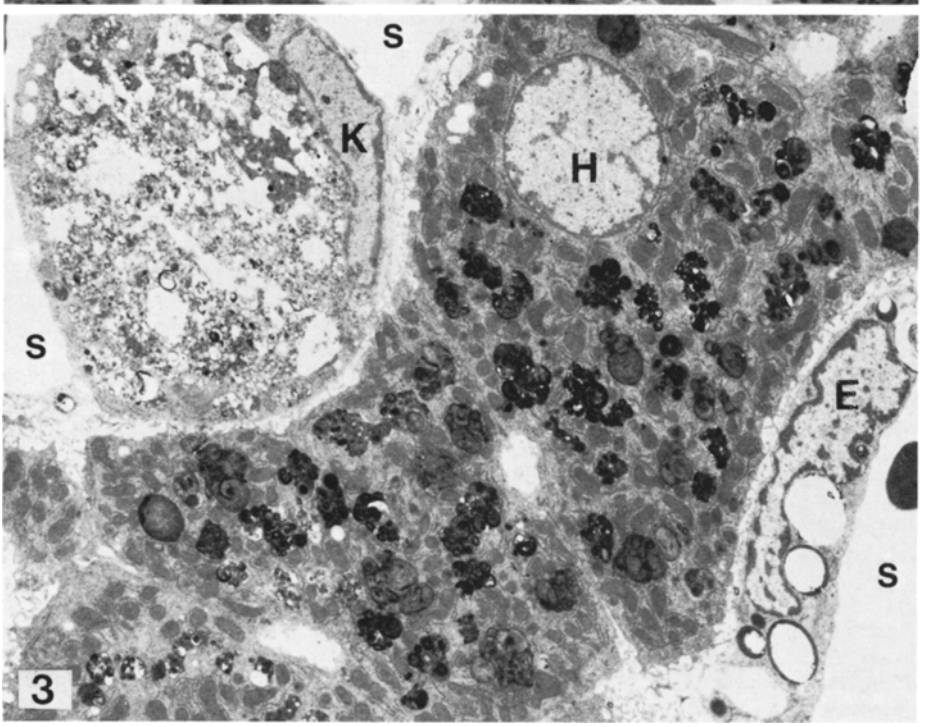

Fig. 2. Micrograph of the liver of a rat treated with tilorone (11 wk, 60 mg/kg × day). The sinusoidal endothelial cells show empty vacuoles. In Kupffer cells the vacuoles are either empty or contain pale-staining material. Hepatocytes show dense cytoplasmic inclusions. Araldite section, stained with toluidine blue-pyronin. × 640

Fig. 3. Low-power electron micrograph of the liver of a rat treated with tilorone (11 wk, 60 mg/kg × day). The endothelial cell has clear vacuoles; the Kupffer cell shows vacuoles containing heterogeneous material; the hepatocytes display numerous lamellated inclusions. × 4,000. *Abbreviations* used throughout the illustrations: *D*, space of Disse; *E*, endothelial cell; *H*, hepatocyte; *K*, Kupffer cell; *S*, sinusoidal lumen

Results

In rats treated with tilorone, the following pathological features were immediately apparent upon light microscopic examination of routine semithin sections (Fig. 2). Sinus endothelial and Kupffer cells throughout the liver lobule contained many clear vacuoles; in addition, Kupffer cells showed vacuoles filled with a material which stained pink or pale-blue with toluidine blue at alkaline pH. Clear vacuoles were also numerous in endothelial cells of larger blood vessels and in the fibroblasts of periportal connective tissue. In the hepatocytes numerous dense inclusions were visible. This pattern of cellular alterations was consistently found in all tilorone-treated rats. The extent of these changes increased with the duration of drug treatment.

Ultrastructurally (Figs. 3, 4), the vacuoles in endothelial cells closely resembled those described in the splenic sinus endothelium (Lüllmann-Rauch 1982a). They contained remnants of an electron-dense matrix adherent to the limiting membrane, while the remaining intravacuolar space appeared entirely empty. Kupffer cells (Fig. 4b) showed various vacuoles, some resembling those in endothelial cells, others containing flocculent material and loosely arranged lamellated structures. In addition, there were vacuoles which contained polymorphic material and also some sharply defined empty spaces. Fat-storing cells (Ito cells) were comparatively rare and displayed some abnormal vacuoles containing granular material. Hepatocytes showed numerous compact lamellated inclusions as described by Leeson et al. (1976); the hepatocytes located next to the central veins and to the periportal fields displayed, in addition to lamellated inclusions, small membrane-bound vacuoles, either empty or containing small amounts of flocculent and membraneous materials (Fig. 4c).

Enzyme histochemistry. Experiments to demonstrate acid phosphatase and trimetaphosphatase gave similar results. Both enzymes could be demonstrated most readily in the lamellated inclusions in hepatocytes (Fig. 5a). In endothelial and Kupffer cells (Fig. 5a, b) some vacuoles were also found containing heavy lead precipitates. In many sinusoidal wall cells the vacuoles were without reaction product.

Endocytosis experiments. As another attempt to test whether or not the abnormal vacuoles were functional parts of the lysosomal apparatus, iron dextran was injected since this electron-dense tracer is known to be taken up by endocytosis and delivered to the lysosomes (Daems et al. 1969). Light microscopic staining for iron revealed that the cellular distribution pattern of the tracer throughout the liver lobule was similar in control rats and tilorone-treated rats, both 24 h and 4 days after the injection of the tracer. Ultrastructurally, the tracer was found within many vacuoles of Kupffer and endothelial cells and also in the lamellated inclusions of hepatocytes. Within the clear vacuoles (Fig. 6), the tracer was always located in the electron-dense matrix at the periphery, while the rest of the intravacuolar space remained empty.

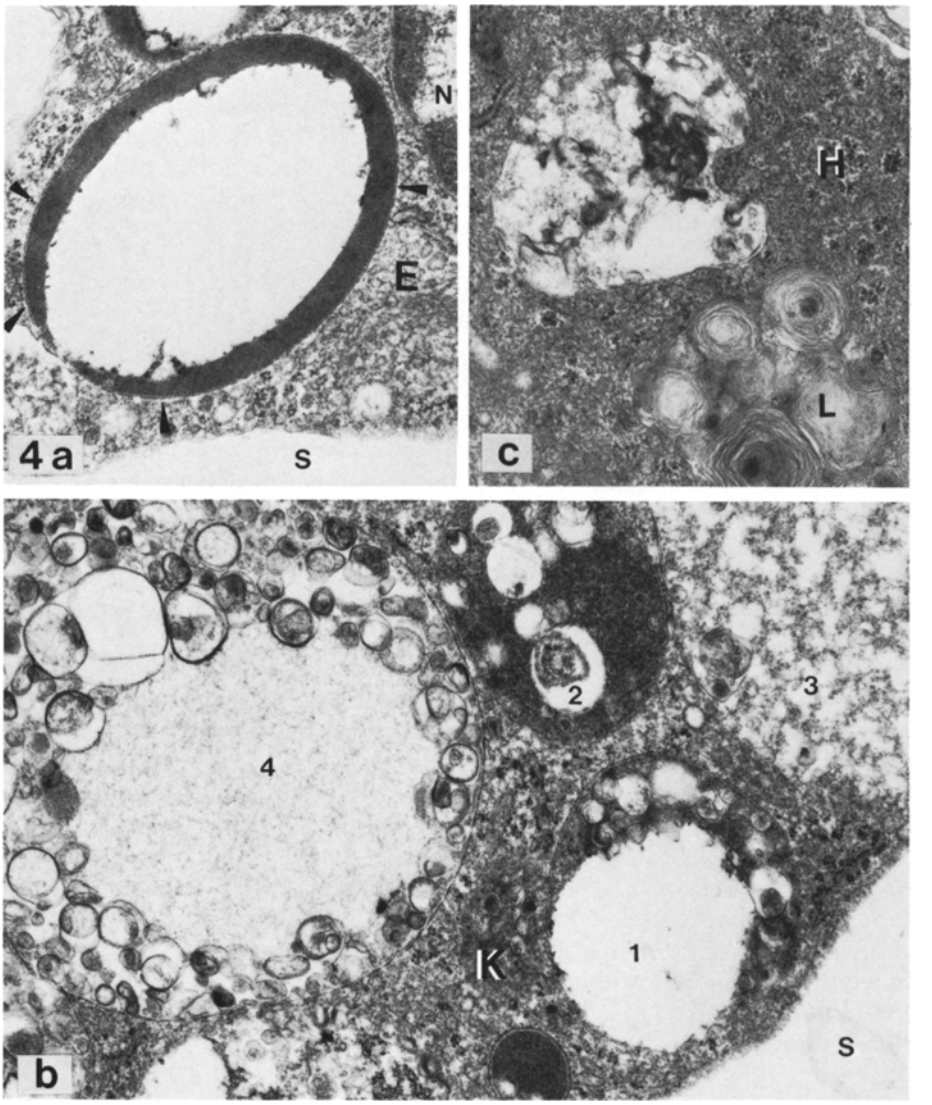

Fig. 4. a Portion of the same endothelial cell as in Fig. 3. The vacuole appears empty except for remnants of an electron-dense matrix adherent to the limiting membrane (*arrowheads*) *N*, nucleus ×22,600. **b** Various types of vacuoles in a Kupffer cell from the same animal as in Fig. 3. Vacuoles 1 and 2 display empty areas within the electron-dense matrix; vacuole 3 contains flocculent material; vacuole 4 is filled with electron-lucent granular material and lamellated structures. ×22,600. **c** Vacuole and lamellated inclusion *L* in a hepatocyte which was located near a periportal field. (Tilorone 6 wk, 60 mg/kg). The vacuole contains flocculent materials of various electron-densities. ×22,600

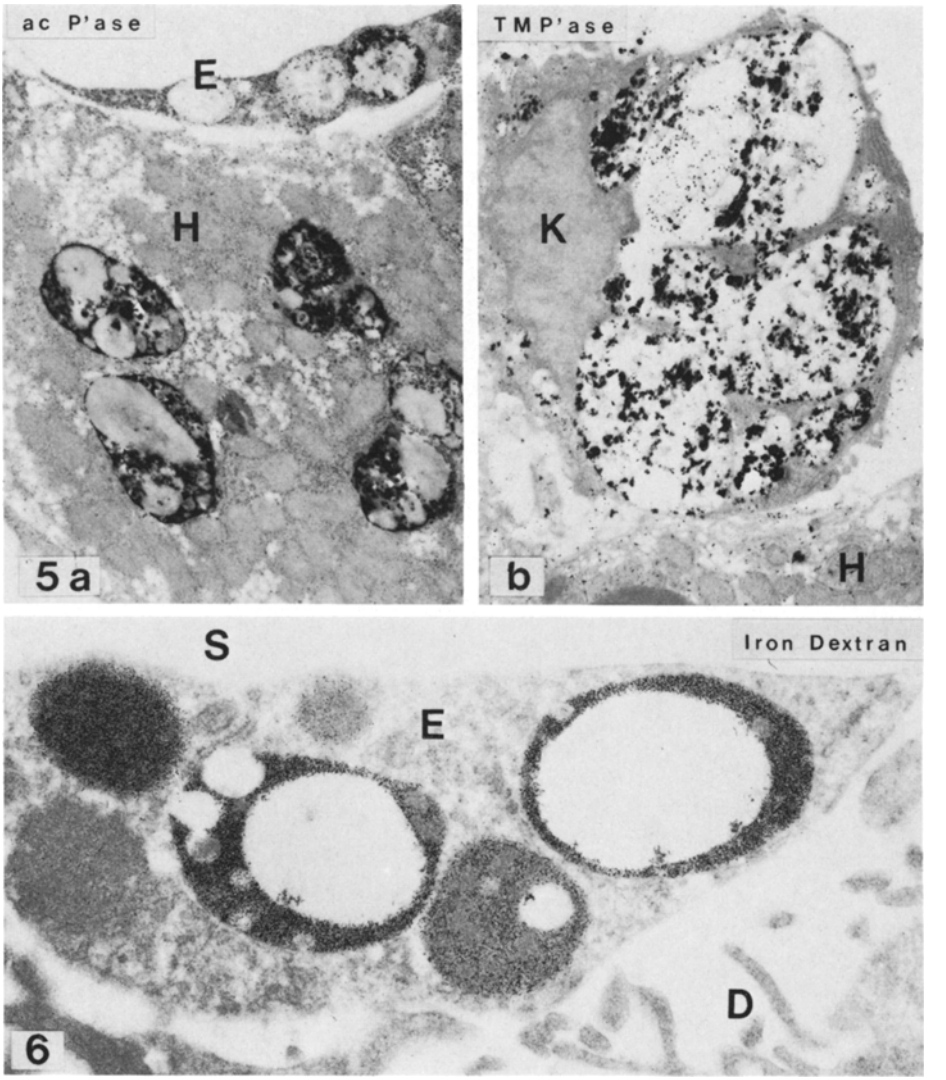

Fig. 5a. Demonstration of acid phosphatase; liver of a rat treated with tilorone (8 days, 4 × 300 mg/kg). Lead precipitates are seen in the lamellated inclusions of the hepatocyte and in one vacuole of the sinus endothelial cell. **b** Demonstration of trimetaphosphatase in the vacuoles of a Kupffer cell from a rat treated with tilorone (3 wk, 60 mg/kg × day). **a**, **b** × 7,400. Unstained sections

Fig. 6. Liver of a rat treated with tilorone (21 wk, 60 mg/kg × day). Iron dextran (Fe 10 mg/100 g body weight) was injected i.v. 24 h before tissue fixation. The electron-dense tracer is found in the tilorone-induced vacuoles. Unstained section. × 22,600

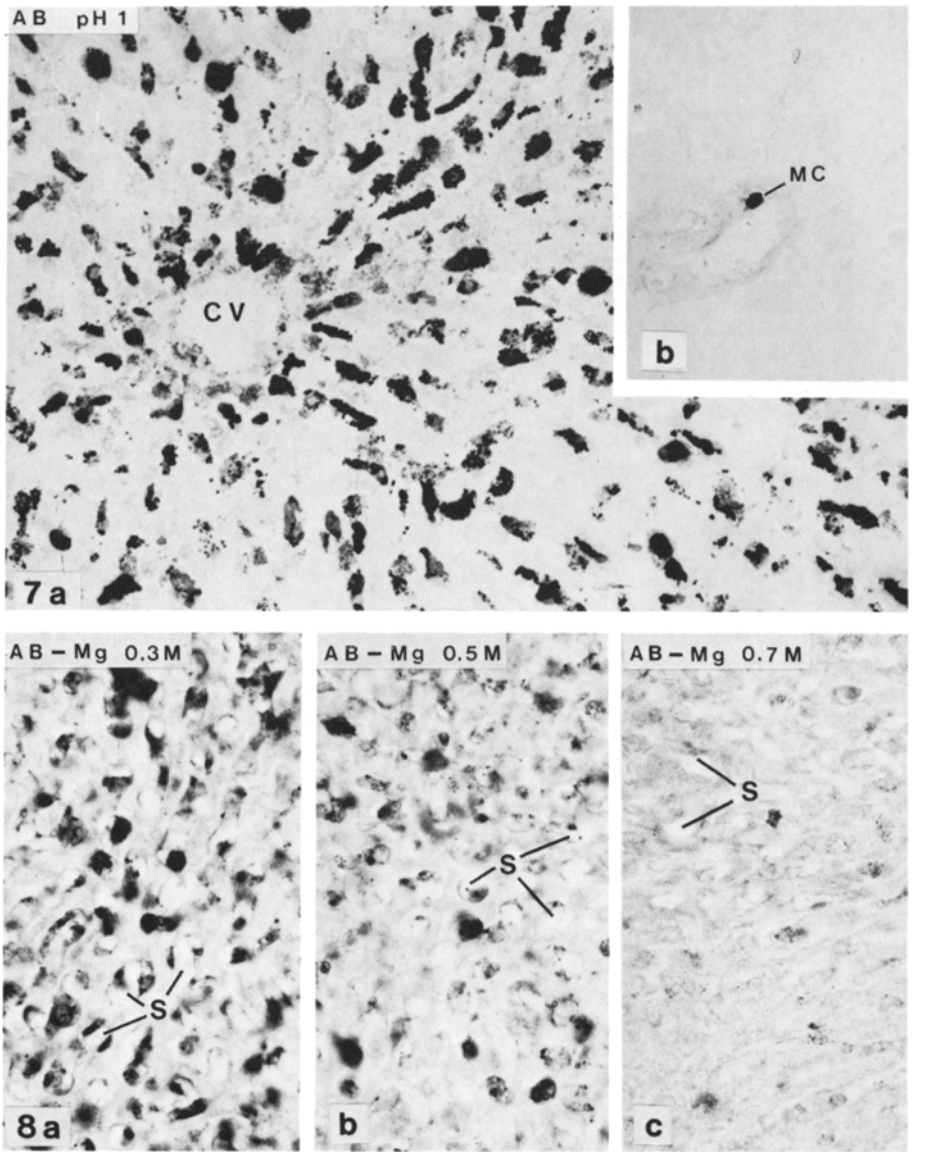

Fig. 7a, b. Cryostat sections stained with Alcian blue (pH 1). **a** Liver of a rat treated with tilorone (13 wk, 60 mg/kg × day). The sinusoidal wall cells are intensely stained. Some hepatocytes near the central vein *CV* show faint granular staining. × 220. **b** Liver of an untreated control rat. The only stained structure is a mast cell *MC* in a periportal field. × 220

Fig. 8. Liver of a rat treated with tilorone (12 wk, 60 mg/kg × day). Slices (40 μm) of glutaraldehyde-fixed tissue were incubated with Alcian blue (pH 5.8) plus $MgCl_2$ (molar concentrations indicated). Sinusoidal wall cells are stained up to a $MgCl_2$ concentration of 0.5 M; at 0.7 M no clear staining is achieved. **a**, **b**, **c**, × 320

Substrate histochemistry

a) *Cryostat sections stained with cationic dyes.* Alcian blue (AB) at pH 1 gave a brillant granular staining of the sinusoidal wall cells (Fig. 7). The intensity of staining and the size of the granules clearly increased with the duration of drug treatment. AB-positive granules were also seen in many cells of the periportal connective tissue and in the endothelium of larger blood vessels. Most hepatocytes remained unstained; only in the periphery and centre of liver lobules, some hepatocytes showed granular staining. In control rats, liver tissue was completely devoid of AB-positive structures at pH 1, except for mast cells in the periportal connective tissue (Fig. 7b).

Staining with toluidine blue at pH 2 yielded basically the same pattern as with AB. In detail, endothelial cells displayed metachromatic (purple) granules; Kupffer cells showed blue and purple inclusions; with increasing time of tilorone treatment (1 to 21 weeks), the proportion of blue to metachromatic inclusions clearly shifted towards the latter. Hepatocytes in the lobular periphery and centre displayed small blue and purple granules; the remaining hepatocytes were as faintly stained as those of control rats. The cytoplasm of sinusoidal wall cells of controls was not stained at all. The only metachromatic (purple) structures present in controls were periportal mast cells.

Extraction experiments showed that the abnormal material staining intensely with AB was highly water-soluble (0.9% NaCl solution) but resistent to treatment with mixtures made up mainly of organic solvents (see Methods). Attempts to preserve the material from extraction by aqueous media were without success as already described in Methods. Enzyme digestion experiments for further characterizing the biochemical nature of the storage materials were unsuccessful for the same reason.

(b) Tissue slices incubated with cationic dyes. Incubation of tissue slices (40 μm) with toluidine blue (pH 2) gave results very similar to those obtained with cryostat sections. The inspection of tissue slices, which were more favourable than cryostat sections for discriminating between endothelial and Kupffer cells, confirmed the rather homogeneous population of metachromatic inclusions in endothelial cells, in contrast to a mixed population of blue and metachromatic inclusions in Kupffer cells. Occasionally, both types of staining were seen in the same inclusion.

AB staining was performed according to Scott and Dorling (1965) for determining the "critical electrolyte concentration" in order to further characterize the polyanionic nature of the storage material (Fig. 8). Sinus endothelium and Kupffer cells showed brillantly staining inclusions up to a $MgCl_2$ concentration of 0.5 M. Staining intensity was greatly reduced at 0.7 M $MgCl_2$ and was totally abolished at 0.9 M $MgCl_2$. For comparison, cartilage stained intensely up to 0.5 M $MgCl_2$ and remained unstained at 0.7 M $MgCl_2$.

(c) High iron diamine method (HID). The HID method of Spicer et al. (1978) for the demonstration of sulfated polyanions gave consistently posi-

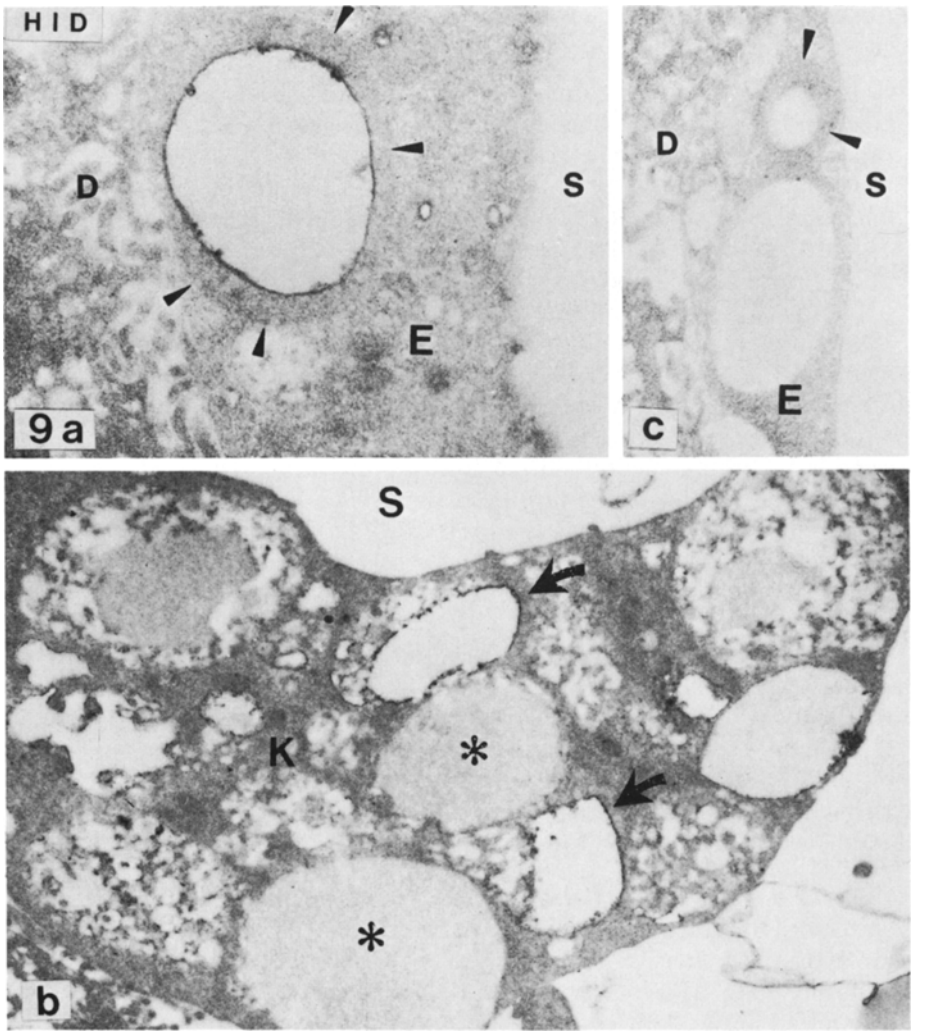

Fig. 9a–c. Liver of a rat treated with tilorone (7 wk, 4 × 300 mg/kg and 17 × 75 mg/kg). High iron diamine procedure (HID), unstained sections. **a** Sinus endothelial cell; within the vacuole positive staining is found at the sharp edge between the clear space and the remnants of the lysosomal matrix. *Arrowheads* point to the membrane of the vacuole. × 22,600. **b** Kupffer cell; some vacuoles show the same pattern of positive staining as seen in the endothelial cell (*arrows*). Some vacuoles which are filled with an electron-lucent material remain unstained (*asterisk*). × 11,500. **c** Endothelial cell from a control preparation incubated in a medium containing $MgCl_2$ instead of $FeCl_3$. No staining is obtained. × 24,700

tive results in the clear vacuoles of sinus endothelial cells and Kupffer cells (Fig. 9). A narrow rim of electron-dense precipitate was found at the sharp border between the dense matrix and the empty space of the vacuoles. In contrast, those vacuoles in Kupffer cells that were filled with polymorphic material without showing any empty areas, were unstained or inconsistently stained by the HID method.

(d) PAS-staining. With both methods used, Kupffer cells displayed PAS-positive inclusions. Endothelial cells remained unstained.

Recovery experiments

After discontinuance of tilorone treatment, the lysosomal storage phenomena faded at greatly differing rates. The lamellated inclusions in hepatocytes largely disappeared within 2 to 4 weeks, which corresponds to previous experience with lipidosis induced by other drugs (Lüllmann-Rauch 1979). In contrast, the vacuoles in sinusoidal wall cells were hardly reduced after a drug-free interval of 7 weeks, and were still present, though less numerous, after 15 weeks.

Discussion

Considerations concerning the storage materials. Two types of lysosomal storage phenomena were observed in tilorone-treated rats. Lipidosis was most conspicuous in hepatocytes, less so in Kupffer cells and absent from endothelial cells. Mucopolysaccharidosis was most prominent in endothelial cells, Kupffer cells, fibroblasts, and was probably also present in the hepatocytes adjacent to central veins and periportal triads. The vacuoles in fat-storing cells cannot be judged on the basis of the present results. The diagnosis of lipidosis is based on the ultrastructural similarities between the lamellated inclusions induced by tilorone and those produced by many other amphiphilic cationic drugs, for some of which lipidosis was also demonstrated biochemically (Lüllmann-Rauch 1979). The diagnosis of mucopolysaccharidosis is based on the histochemical findings. They provide evidence for lysosomal storage of polyanionic water-soluble materials which have staining characteristics of sulfated GAG. The determination of the critical electrolyte concentration according to Scott and Dorling (1965) indicated that the polyanionic character of the storage materials in sinusoidal wall cells was similar to that of cartilagineous GAG, and slightly less acidic than the abnormal material stored in the splenic sinus endothelium of tilorone-treated rats (Lüllmann-Rauch 1982a). A more detailed diagnosis concerning the particular types of aGAG could not be achieved as explained in Methods; this problem has to be tackled biochemically.

The present findings suggest some differences with respect to the polyanionic materials stored in the sinus endothelium and in Kupffer cells. In the endothelium, the predominant metachromatic staining with toluidine blue (pH 2), the consistent HID stainability and the invariable ultrastructural picture of the clear vacuoles suggest that the storage material was rather homogeneously composed of sulfated GAG. In contrast, the vacuoles in Kupffer cells were heterogeneous in their ultrastructure and in their histochemical staining characteristics. It appears likely that, in addition to storing sulfated GAG, they contained other non-sulfated anionic materials such as acidic glycoproteins ultrastructurally represented by flocculent HID-negative material; this is also suggested by the presence of PAS-positive inclusions in Kupffer cells.

Comparison with inherited mucopolysaccharidoses. The basic potency of tilorone to induce generalized mucopolysaccharidosis is also indicated by some preliminary findings on urinary excretion of aGAG. The urine of chronically treated rats contained abnormal metachromatic material (B. Christensen and G. Michel, personal communication) as demonstrated by Berry's spot test (Spranger and v. Germar 1967); the excreted hexuronic acids per gram of creatinine were increased 20-fold compared with the control (J. Gehler, personal communication). Further studies are necessary to elucidate the exact biochemical nature of the excreted materials and of those stored in liver and other organs.

Concerning the cellular pattern of GAG storage, the tilorone-induced condition does not directly mimic a particular type of the inherited mucopolysaccharidoses. In several types, the hepatocytes are heavily vacuolated (Van Hoof 1973), which was not a prominent feature in tilorone-treated animals. On the other hand, the vacuolation in Kupffer cells was reminiscent of the descriptions in most types of inherited aGAG storage diseases. Sinus endothelial cells are rarely mentioned in this context; in two cases of chondroitine-4-sulfate storage (Freitag et al. 1971) and in a case of type IV (Morquio's disease) (Wisse et al. 1974) the sinus endothelia were described as having numerous clear vacuoles.

Considerations on the mechanisms of the drug side effects. In view of previous experience with at least 30 other amphiphilic cationic drugs it appears reasonable to explain tilorone-induced lipidosis by the same mechanism as proposed previously, i.e. by drug-lipid interaction leading to interference with intralysosomal lipid digestion (Lüllmann et al. 1978). As to aGAG storage, a preliminary finding suggests that this also is due to decreased degradation rather than to increased synthesis. In tilorone-exposed cultured human fibroblasts the kinetics of sulfate degradation (Fratantoni et al. 1968) were similar to those in fibroblasts from individuals with inherited mucopolysaccharidosis (K. v. Figura, personal communication). This observation is reminiscent of the effects of other weak bases such as chloroquine upon the sulfate kinetics of cultured cells (Lie and Schofield 1973; Glimelius et al. 1977).

The molecular mechanisms responsible for decreased aGAG degradation are entirely open to speculation at present. Obviously, there is a dissociation between the potencies to induce lipidosis and mucopolysaccharidosis: among all cationic amphiphilic drugs so far investigated, tilorone is the only compound producing both storage phenomena in intact organisms. It appears reasonable to assume that tilorone is a "lysosomotropic" drug like chloroquine and other weak bases (DeDuve et al. 1974), and that this property is somehow related to the lysosomal side effect under debate here. It is tempting to speculate that the drug interferes with the supply of newly synthesized enzymes towards the lysosome as has been described in chloroquine-exposed cultured fibroblasts (Gonzalez-Noriega et al. 1980; Hasilik and Neufeld 1980; Neufeld 1981; Sly et al. 1981). It should, however, be

emphasized that we have not so far found any morphological signs that chloroquine, although producing severe lipidosis, would induce mucopolysaccharidosis-like alterations in the liver or any other organ of the intact rat comparable to those seen with tilorone. Thus it remains unclear to which extent the concept of Sly et al. (1981) is applicable to explain the alterations found with tilorone under in vivo conditions. Further studies are now in progress to elucidate the molecular drug characteristics required to induce lysosomal aGAG storage.

Acknowledgements. Thanks are due to Dagmar Niemeier for excellent technical assistance throughout this study, to Heidrun Hansen and Ursula Frischkorn for skilful help with the histochemical work, and to Heide Siebke and Heidi Waluk for the photographical work.

References

Daems WT, Wisse E, Brederoo P (1969) Electron microscopy of the vacuolar apparatus. In: Dingle JT, Fell HB (eds). Lysosomes in biology and pathology, Vol 1. North-Holland, Amsterdam, pp 64–112

De Duve C, De Barsy T, Poole B, Trouet A, Tulkens P, Hoof F Van (1974) Lysosomotropic agents. Biochem Pharmacol 23:2495–2531

Doty SB, Smith CE, Hand AR, Oliver C (1977) Inorganic trimetaphosphatase as a histochemical marker for lysosomes in light and electron microscopy. J Histochem Cytochem 25:1381–1384

Fratantoni JC, Hall CW, Neufeld EF (1968) The defect in Hurler's and Hunter's syndromes: Faulty degradation of mucopolysaccharide. Proc Natl Acad Sci USA 60:699–706

Freitag F, Küchemann K, Schuster W, Spranger J (1971) Hepatic ultrastructure in chondroitin-4-sulfate mucopolysaccharidosis. Virchows Arch [Cell Pathol] 8:1–15

Glimelius B, Westermark B, Wasteson A (1977) Ammonium ion interferes with the lysosomal degradation of glycosaminoglycans in cultures of human glial cells. Exp Cell Res 108:23–30

Gonzalez-Noriega A, Grubb JH, Talkad V, Sly WS (1980) Chloroquine inhibits lysosomal enzyme pinocytosis and enhances lysosomal enzyme secretion by impairing receptor recycling. J Cell Biol 85:839–852

Hasilik A, Neufeld EF (1980) Biosynthesis of lysosomal enzymes in fibroblasts. Synthesis as precursors of higher molecular weight. J Biol Chem 255:4937–4945

Ito S, Winchester RJ (1963) The fine structure of the gastric mucosa in the bat. J Cell Biol 16:541–577

Leeson GA, Biedenbach SA, Chan KY, Gibson JP, Wright GJ (1976) Decrease in the activity of the drug-metabolizing enzymes of rat liver following the administration of tilorone hydrochloride. Drug Metab Dispos 4:232–238

Levine S, Sowinski R (1977) T-lymphocyte depletion and lesions of choroid plexus and kidney induced by tertiary amines in rats. Toxicol Appl Pharmacol 40:147–159

Lie SO, Schofield B (1973) Inactivation of lysosomal function in normal cultured human fibroblasts by chloroquine. Biochem Pharmacol 22:3109–3114

Lüllmann H, Lüllmann-Rauch R, Wassermann O (1978) Lipidosis induced by amphiphilic cationic drugs. Biochem Pharmacol 27:1103–1108

Lüllmann-Rauch R (1979) Drug-induced lysosomal storage disorders. In: Dingle JT, Jacques PJ, Shaw IH (eds). Lysosomes in applied biology and therapeutics, vol 6. North Holland, Amsterdam, pp 49–130

Lüllmann-Rauch R (1982a) Histochemical evidence for lysosomal storage of acid glycosaminoglycans in splenic cells of rats treated with tilorone. Histochemistry 76:71–87

Lüllmann-Rauch R (1982b) Lysosomal glycogen storage mimicking the cytological picture of Pompe's disease as induced in rats by injection of an α-glucosidase inhibitor. II. Alterations in kidney, adrenal gland, spleen and soleus muscle. Virchows Arch [Cell Pathol] 39:187–202

Mayrhofer G (1980) Fixation and staining of granules in mucosal mast cells and intraepithelial lymphocytes in the rat jejunum, with special reference to the relationship between the acid glycosaminoglycans in the two cell types. Histochem J 12:513–526

Neufeld EF (1981) Recognition and processing of lysosomal enzymes in cultured fibroblasts. In: Callahan JW, Lowden JA (eds). Lysosomes and lysosomal storage diseases. Raven Press, New York, pp 115–129

Oliver C (1980) Cytochemical localization of acid phosphatase and trimetaphosphatase activities in exocrine acinar cells. J Histochem Cytochem 28:78–81

Pearse AGE (1961) Histochemistry-theoretical and applied. 2ed Little, Brown & Co, Boston

Regelson W (1981) The biological activity of the synthetic polyanion, pyran copolymer (diveema, MVE, 46015) and the heterocyclic bis DEAE fluorenone derivative, tilorone and congeners: clinical and laboratory effects of these agents as modulators of host resistance. Pharmacol Ther 15:1–44

Scott JE, Dorling J (1965) Differential staining of acid glycosaminoglycans (mucopolysaccharides) by Alcian blue in salt solutions. Histochemie 5:221–233

Scott JE, Quintarelli G, Dellovo MC (1964) The chemical and histochemical properties of Alcian blue. I. The mechanism of Alcian blue staining. Histochemie 4:73–85

Sly WS, Natowicz M, Gonzalez-Noriega A, Grubb JH, Fischer HD (1981) The role of the mannose-6-phosphate recognition marker and its receptor in the uptake and intracellular transport of lysosomal enzymes. In: Callahan JW, Lowden JA (eds). Lysosomes and lysosomal storage diseases. Raven Press, New York, pp 131–146

Spicer SS, Hardin JH, Setser ME (1978) Ultrastructural visualization of sulphated complex carbohydrates in blood and epithelial cells with the high iron diamine procedure. Histochem J 10:435–452

Spranger J, Germar R v. (1967) Mucopolysaccharid-Suchtest. Clin Pediatr 6:659–660

Thelmo WL, Levine S (1978) Renal lesions induced by tilorone and an analog. Am J Pathol 91:355–360

Van Hoof F (1973) Mucopolysaccharidoses. In: Hers GH, Van Hoof F (eds). Lysosomes and storage diseases. Academic Press, New York, pp 217–259

Weiss JN, Weinberg RS, Regelson W (1980) Keratopathy after oral administration of tilorone hydrochloride. Am J Ophthalmol 89:46–53

Wisse E, Emeis JJ, Daems WT (1974) Some fine structural considerations on the possible involvement of the liver RES in lysosomal storage diseases, with observations in a case of Morquio's disease. In: Tager JM, Hooghwinkel GJM, Daems WT (eds). Enzyme therapy in lysosomal storage diseases. North-Holland, Amsterdam, pp 95–109

Received July 25 / Accepted August 8, 1983